UNIVERSITY OF CALIFORNIA SAN DIEGO

Development of Mouse Brown Adipose Tissue During Perinatal Period

A Thesis submitted in partial satisfaction of the requirements for the degree Master of Science

In

Biology

By

Samuel Lee

Committee in charge:

Jianhua Shao, Chair
Elina Zuniga, Co-Chair
Stanley Lo

2018

The Thesis of Samuel Lee is approved, and it is acceptable in quality and form for publication on microfilm and electronically:

_____

_____ Co-Chair

_____ Chair

University of California San Diego

2018

DEDICATION

I dedicate this thesis to all those who were a part of Shao Lab, especially Jean-Sebastian Wattez and Liping Qiao for their support and guidance.

TABLE OF CONTENTS

LIST OF FIGURES

ACHNOWLEDGEMENTS

I would like to acknowledge Dr. Shao for providing me the experience, mentorship, trust, and understanding to fruitfully conduct scientific research. I am truly grateful for not only how he treated me as an academic, but how he fostered an interest in science within me. I will forever remember the lessons he's taught me.

I would also like to thank my committee members, Dr. Elina Zuniga and Dr. Stanley Lo, for their dedication, patience, and support in their roles as committee members.

I would like to thank Jean-Sebastian Wattez, known as "JS" at our lab. His direct mentorship and thoughtful discussions taught me the techniques needed to pursue my scientific career.

I would like to extend special thanks to Liping Qiao for her dedication and wholesome a ethic. Working with her I picked up her habits of organization, skillful operation, and most importantly appreciation for science. I am honored to have had the opportunity to work with Liping.

Lastly, I would like to thank the rest of the members of the Shao Lab for their inquisitive questions and lively conversations that sharpened my wit and scientific progress.

ABSTRACT OF THE THESIS

Development of Mouse Brown Adipose Tissue During Perinatal Period

by

Samuel Lee

Master of Science in Biology

University of California San Diego, 2018

Professor Jianhua Shao, Chair
Professor Elina Zuniga, Co-Chair

Although brown adipose tissue (BAT) has recently become a topic of interest due to its newfound presence in adult humans, the morphology brown adipocytes and expression of uncoupling protein 1 (UCP1) during developmental embryonic and postpartum time frames

remains unclear. Additionally, little is known about how maternal obesity affects BAT development in fetal offspring. We selected pups of C57BL/6J dams from E15.5 through P30.5 under standard pregnancy conditions. Interscapular BAT (iBAT) samples were taken and analyzed using hematoxylin and eosin staining, western blotting for anti-UCP1, and fluorescent imaging using UCP1-creER mT/mG transgenic construct. We placed C57BL/6J dams on 60% high fat calorie content diets 3 months before gestation and analyzed UCP1 content in pups using immunohistochemistry for anti-UCP1. Analysis on pup iBAT during standard pregnancies along our perinatal time frame revealed a linearly significant decrease in cell density and increase in adipocyte area. Moreover, both iBAT mass ratio to body weight and UCP1 protein expression spiked on P0.5 and eventually diminished. UCP1-creER mT/mG fluorescent imaging revealed UCP1 gene activity as early as E18.5. Maternal obesity increased UCP1 expression in iBAT at birth. Our study provides foundational information into the structural morphology of perinatal iBAT and the starting time point of UCP1 expression. We also find maternal obesity causes an increase in UCP1 expression during postpartum development in pups.

Introduction

Background on Obesity:

Obesity is a currently a widespread epidemic in the United States and globally. According to the World Health Organization, obesity is defined as having a body mass index in excess of 30 kg/m^2. Individuals at or beyond this level are prone to diseases associated with severe obesity, including but not limited to type 2 diabetes, cardiovascular disease, and cancer (Wilding 2001). As of 2015, obesity affected 36.5% of all American adults and nearly 17% of American children (Ogden 2015). Worldwide, surveys conducted between 1990-2010 in over 40 countries estimate that more than 2 billion people are overweight or obese (Popkin 2012). In developing nations, this is very likely due to increased sugar consumption, where both physical inactivity and sugar consumption were significant predictors of hypertension brought on by obesity (Hanson 2014). With the introduction of technology and a growing interdependence on advanced nations, developing nations are replacing diets that once consisted of legumes, vegetables, and coarse grains for Western-style diets rich in processed carbohydrates, animal fats, and added caloric sweeteners. Overall, urban areas show a higher prevalence of obesity compared to rural areas. But recent studies suggest that the annual increase in obesity in women from rural areas (3.9%) outpaces that of obesity in women from urbanized settings (2.5%) (Popkin 2012). Despairingly, there shows no indication of a decline in this epidemic - with obesity rates in adults and children remaining similar between 2003-2004 and 2011-2012 (Ogden 2014). As of 2008, it cost the US $147 billion in Medicaid and Medicare to treat obesity related diseases, which is around 9% of all medical expenditures (Finkelstein 2009). To further compound this epidemic, estimates suggest as much as a 33% increase in obesity and a 130% increase in severe obesity may be expected by 2030. In terms of the number of people affected, it

is estimated that an astonishing 51.1% of American adults or roughly 1.12 billion people will be obese (Finkelstein 2012, Kelly 2008). Perhaps most alarming is the state of childhood obesity. In the US alone, childhood obesity rates have increased to 3.3-fold over the past two decades. Globally, these trends remain apparent with Haiti increasing 3.5-fold, Egypt increasing 3.9-fold, Brazil increasing 3.6-fold, and Australia increasing 4.6-fold over a 10 year period (Ebbeling 2002). Along with an unprecedented increased diagnosis of childhood type 2 diabetes, obesity in adolescents is detrimental to their long term development and growth due to aberrant hormonal changes (Copeland 2005, Dunger 2005).

This level of obesity will take its toll financially on the healthcare system with over $956 billion or 17.6% of all healthcare costs projected to be spent treating obesity related illnesses by 2030 (Wang 2008). Globally, obesity is the fifth leading cause of death and claims nearly 208 million adult lives annually (Hanson 2014).

Though current evidence clearly illustrates the obesity epidemic as a growing dilemma, the factors responsible are multifaceted. At its basis, energy used by the body is stored in the form of lipids in white adipose tissue (WAT). WAT is an adaptive organ capable of undergoing lipolysis, lipogenesis, glucose uptake, and synthesis of triglycerides to accommodate metabolic stasis (Ràfols 2014). WAT is also the largest endocrine organ comprising up to 20% of body mass in healthy individuals and 50% of body mass in obese individuals. It produces various hormonal adipokines like leptin, adiponectin, visfatin, resistin, chemerin - all of which are significant regulators of angiogenesis, blood pressure, glucose homeostasis, vascular hemostasis, and lipid metabolism (Hassan 2012). White adipocytes in obese patients show increased number of cells (hyperplasia) and volume per cell (adipocyte hypertrophy) (Nakamura 2014). Indeed, WAT is an important evolutionary development to ensure adequate energy storage and

expenditure of this energy for survival. Though numerous factors have been shown to increase the risk of obesity, the consensus is that obesity is caused by an imbalance in energy homeostasis. Excessive energy intake and suboptimal energy expenditure are at the forefront of the obesity epidemic. The introduction of processed, highly caloric, largely portioned, and relatively inexpensive foods have swamped grocery stores, vending machines, and restaurants - altogether contributing to a culture of overnutrition and subsequently excessive energy intake (Wright 2012). Other sources of obesity come from a decrease in physical activity or energy expenditure. In 2005, nearly half of all adults and adolescents in the US did not meet physical activity standards (Wright 2012). This was due in part to the advent of sedentary lifestyles brought on by technological advances in blue-collar work automation, leisure, food production, and disinterest in behaviors that endorse physical activity (Finkelstein 2010). Additional sources suggest increased stress and anxiety, inadequate sleep, higher socioeconomic status, genetics, and social networks work interconnectedly and contribute to the obesity epidemic (Egger 2014).

For these reasons, obesity has become an alarming health issue. Obesity as a risk factor for type 2 diabetes has been widely investigated. Obesity, or elevated adiposity, leads to increased release of non-esterified fatty acids (NEFA) into the blood serum. Elevated serum NEFA causes insulin resistance, whereby cellular processes of glucose transport, glycogen synthesis, and lipogenesis are severely inhibited (Boden 2011). As the demand for glucose across all organs increases because of insulin resistance, glucotoxicity develops due to hyperglycemia. This ultimately results in pancreatic beta cell death, whereby insulin is insufficient - the hallmark of type 2 diabetes (Cnop 2005). Importantly, obesity correlates with an increased risk of hypertension. Obese patients are three times as likely to develop hypertension when compared to normal weight patients (Kearney 2005). Accordingly, cardiovascular diseases show strong links

with obesity. Obese men are 72% more likely to develop coronary heart disease (Rimm 1995). Augmented adipocytes secrete proinflammatory adipokines that, in addition to glucotoxicity and insulin resistance, greatly increase the risk of cardiovascular disease (Bastien 2014). Obesity is also a leading risk factor in cancer, with 13% of cancer cases worldwide and 20% in the US and Europe attributed to obesity (Allott 2015). Overweight and obese adolescents show a 40% increased likelihood of developing pancreatic cancer later in life (Genkinger 2015). Similarly, obese women showed a 58% increased risk of invasive breast cancer. Deaths resulting from breast cancer were two-fold greater in obese women compared to normal BMI women (Neuhouser 2015). While the exact link between obesity and cancer remain elusive, theories involving proinflammatory adipokines and metabolic symbiosis between cancer cells and adipocytes show promise (Park 2014).

Background on BAT and UCP1:

Aside from WAT, mammals exhibit another form of adipocyte known as brown adipose tissue (BAT). BAT differs significantly from WAT in both form and function. Though both adipose tissues store triglycerides via intracellular lipid deposits, BAT has multilocular lipid droplets allowing for faster metabolism compared to WAT's unilocular droplets (Enerbäck 2010, Oelkrug 2015). This rapid utilization of energy allows for BAT's unique function in non-shivering thermogenesis to produce heat rather than ATP (Klingenspor 2017). As its namesake, BAT is brown in color due to an abundance of specialized mitochondria that have been modified such that oxidative phosphorylation uncouples hydrogen (Rafael 1976). Specifically, upon cold exposure, BAT is activated by sympathetic nerve action. This leads to the activation of b-adrenergic signaling pathways leading to lipolysis in BAT. The generated free fatty acids then

activate uncoupling protein 1 (UCP1) along the inner membrane of brown adipocyte mitochondria. UCP1 uncouples oxidative phosphorylation from ATP synthase, thereby allowing protons to "short circuit" and flow down a proton gradient bypassing ATP synthase. In doing so, UCP1 uncouples the electromotive force from ATP production and generates heat (Lidell 2014). BAT also utilizes glucose as an energy source from circulating serum. It is capable of a 12-fold glucose uptake in cold conditions and 5-fold uptake under insulin stimulation compared to inactive thermoneutral conditions in adult humans (Townsend 2014). In mice and infant humans, interscapular BAT (iBAT) is a considerable source of BAT and is often studied (Lidell 2014)

Evolutionarily, the ability to generate heat serves to protect against adverse cold climate during nocturnal hours, prolonged hibernation, and hypothermia in mammalian neonates (Cannon 2004, Teruel 1995). Once thought to disappear after neonatal development, BAT has been detected in adult humans through 18 fluoro-deoxyglucose uptake using positron emission tomography and computed tomography (PET/CT) scanning (Chechi 2013). Using this technique current estimates suggest that 50 grams of BAT can account for 20% of all adult metabolic energy expenditure where men have a median of 11.6 grams and women have 12.3 grams, though a maximal mass of 42 grams for men and 170 grams for women have been detected (Cypess 2009). This recent quantification of BAT has led it to be a potential therapeutic target of obesity. BAT is capable of activation and expansion and protects against obesity through cold exposure and diet-induced thermogenesis (Chechi 2013). By augmenting uptake of fatty acids and glucose, BAT improves insulin sensitivity (Townsend 2014). Indeed, BAT has long been known to be cold-inducible. After four weeks of cold-exposure at 10□, BAT expands up to 45% in volume of activity and increases oxidative metabolism by 2.2-fold to overcompensate its heat production in humans (Blodin 2014). Another study indicates that humans subjected to

intermittent cold exposure at 19□ over 36 hours yielded a 5.3% increase in energy expenditure and 10.5% increased BAT activity compared to subjects at room temperature (Chen 2013). Recent studies even point to the presence of WAT inducible browning of adipocytes due to cold exposure, known as beige or brite adipocytes that are capable of non-shivering thermogenesis (Sidossis 2015). An additional function of BAT is to actively protect against excessive energy intake known as diet-induced thermogenesis (Hibi 2016). When presented with high fat diets, BAT-positive subjects showed an increased energy expenditure of 56 kcal/d compared to BAT-negative subjects (Hibi 2016). However, the concept of diet-induced thermogenesis and the role BAT plays in it remains controversial. Methodological inconsistencies in measurement between various studies and lack of evidence that diet-induced thermogenesis existed as an evolutionary benefit to early humans call into question the validity of current research (Kozak 2010, Anouk 2014).

UCP1 is also known as thermogenin and is one of five proteins that work to uncouple oxidative phosphorylation in brown adipocyte mitochondria (Rousset 2004). UCP1 is of interest because it actively regulates thermogenesis, whereas UCP2 and UCP3 take a more passive role in resting metabolic rate (Rousset 2004). Additionally, UCP1 is the only known protein that allows for uncoupling to produce heat through thermogenesis. As such, other UCPs cannot replace UCP1, reaffirming its unique functionality (Nedergaard 2001). UCP1 is embedded within the inner mitochondrial membrane and is comprised of six transmembrane domains in a triplicated structure with every third domain made up of two α-helices and a polar domain (Rousset 2004). Surprisingly, UCP1 is not expressed in any tissue other than BAT, though recent evidence suggests cold-induction of beige adipocytes also express functional UCP1 (Ricquier 2000, Shabalina 2013). UCP1 makes up 4% of BAT mass and 8% of mitochondrial protein mass

(Rousset 2004). It can produce up to 300W/kg in fully stimulated BAT, while other tissues fall short at only 1W/kg (Symonds 2013). UCP1 plays a significant role in regulating metabolic balance and may prove to be of therapeutic benefit in reversing the negative effects of obesity (Brodani 2012). Mice that have UCP1 ablated gained weight at 50% faster rate than wild type mice over 4 months in both control diets and high fat diets at physiological thermoneutrality (Feldmann 2009). Human subjects using a fucoxanthin supplement, a carotenoid found in marine species, show increased resting energy expenditure, leading to a significant reduction in body weight and fat in obese subjects. Interestingly, fucoxanthin highly upregulates UCP1 protein expression and UCP1 mRNA levels, highlighting UCP1's role in mitigating obesity (Gammone 2015).

Background on BAT Development and Activation:

Both brown and white adipocytes originate from the embryonic mesoderm, tracing a common lineage with the development of skeletal muscle, bone, and connective tissue (Gesta 2007). While the exact adipogenic progenitors used in the formation of BAT are yet to be conclusively determined, myogenic factors Myf5, myoD, myogenin are suggested in part to differentiate brown adipocytes (Enerbäck 2010). Additionally, overexpression of transcription factor PR domain containing 16 (PRDM16) has been shown to regulate adipogenic progenitors to differentiate into BAT from myogenic precursors (Kajmura 2009). Similarly, mice with PRDM16 knockdown expressed lower levels of brown adipocyte markers and an increased expression of myogenic transcription factors (Seale 2008). Peroxisome proliferator-activated receptor γ coactivator 1α (PGC-1α) is theorized to initialize BAT thermogenesis after adrenergic signaling due to cold stimulation (Lidell 2014). Mice with PCG-1α knockdown are unable to

produce heat in response to cold induction and lack expression thermogenic genes in response to adrenergic stimulation (Lin 2004). Other regulatory proteins like sirtuin-1 (SIRT1) and steroid receptor coactivators (SRCs) affect the modularity of BAT, allowing for varied thermogenic expression (Lidell 2014).

BAT becomes first distinguishable on embryonic day 15.5 (E15.5) in mice, though delineation between myogenic and brown adipocytes can take place as early as E11.5 (Lepper 2010). BAT persists after this point, gradually expanding in size and morphologically developing until birth (Kaufmans 2016). UCP1 in BAT first appears on E17.5 and gradually increases its expression up until birth (Chabowska-Kita 2016). Mice have 18.5 days of embryonic development, where P0.5 designates birth. Mice develop much of their BAT postpartum with postpartum day 6.5 (P6.5) showing signs of thermogenesis, followed by stable thermogenesis on P15.5 (Newkirk 1995). Altricial species like mice that readily huddle for warmth postpartum have most of their BAT in the interscapular regions, while precocial species like sheep and humans that do not huddle have BAT localized around the kidneys and thoracic regions (Symonds 2015).

BAT development has been robustly studied in precocial sheep ovine species. Histological analysis during mid-gestation of 80 days reveal BAT as a dense mass of cells without distinctive morphology. Moreover, BAT at this stage lack UCP1 as evidenced by immunohistochemistry (Pope 2013). Late-gestation at 140 days reveals rapid development of brown and white adipocytes marked by an increase in protein and lipid mass in these tissues, with maximal UCP1 expression occurring directly after birth (Clarke 1997, Pope 2013). As a precocial species, sheep are capable of activating BAT for non-shivering thermogenesis immediately after birth through both cold exposure and prolactin from maternal lactation

(Symonds 2012). However, by 30 days postpartum, brown adipocytes recede, gradually replaced by white adipocytes. Consequently, UCP1 gene expression is significantly lowered and sustained through the rest of adult life (Symonds 2012). While information on human fetal BAT development requires further investigation, humans and sheep share many similar developmental milestones. Within 20-weeks of gestation, UCP1 expression can be found within depots of adipose tissue, similar to the late-gestational stage of sheep (Velickovic 2014). As with sheep, BAT in humans continues to develop and is maximally expressed at birth. It then loses 50% of its thermogenic output before postpartum day 10 and by adulthood only accounts for 4% of adipose tissue mass (Symonds 2015). This rapid disappearance of human BAT is an area of intense study as BAT is seen as a potential therapeutic strategy to counter obesity.

Background on Fetal Programming:

Throughout pregnancy, the health of the mother affects the health outcomes of offspring even through adulthood. Fetal programming is the ability of pregnant mothers to affect and alter the epigenetics of their offspring, often through environmental changes such as diet (Neri 2015). Pregnant mice have an increased WAT and BAT mass compared to virgin mice. However, measurements of cytochrome oxidase activity indicating mitochondrial activity and GDP-binding indicating thermogenic expenditure were significantly lower in pregnant mice. This suggests a diminished functionality on behalf of BAT during pregnancy, likely to redirect energy resources to developing pups (Trayhurn 1987). While this is overall beneficial for gestation, maternal obesity directed fetal programming leads to postponed health complications for the offspring. Indeed, maternal obesity is widely associated with an increased risk of hypertension, cardiovascular disease, neurological disorders, obesity, diabetes, and other metabolic disorders

during adulthood in infants (Neri 2015). WAT hyperplasia and hypertrophy typical in obesity secrete proinflammatory adipokines have been suggested to negatively impact fetal development and contribute to metabolic and cardiovascular disorders (Segovia 2014). Gestational diabetes mellitus (GDM) is the development of maternal glucose intolerance during pregnancy (Metzger 2007). Though only present in 14% of US pregnancies and often disappears after birth, GDM nevertheless puts both mother and infant at significant risk for developing type 2 diabetes (Ashwal 2015). The underlying pathophysiology of GDM is not fully understood. But current research suggests an interplay of pro-inflammatory adipokines and overexpressed placental hormones to be causative factors (Fasshauer 2014). Insulin insensitivity due to GDM causes maternal hyperglycemia. Left untreated, excess glucose passes through the placenta and enters the embryonic environment stimulating increased fetal insulin production that adversely affects fetal development (Diabetes Care 2003).

Hypothesis/Aim:

Through the recent identification of active human BAT, therapeutic endeavors to offset deleterious effects of obesity are extensively researched. However, the role BAT and subsequently UCP1 play in fetal programming of metabolism is still largely unexplored. Studies do investigate how maternal diet affects the morphology of BAT in adult rat offspring (Santos 2017). However, insight into how maternal diet affects fetal BAT morphology during the developmental perinatal stage is lacking. While UCP1 protein and mRNA have been quantified from neonates, a representative histological visualization has yet to be developed (Budge 2002). We investigate morphological changes in fetal mouse BAT during perinatal development while quantifying UCP1 concentrations. Additionally, we look to histologically visualize UCP1 in fetal

mouse BAT using transgenic UCP1-creER mT/mG mice. Furthermore, we investigate the effects of fetal programming through high fat maternal diet during pregnancy. Though the nature of our experiments is exploratory, we hypothesize that maternal obesity during pregnancy will affect fetal programming by upregulating UCP1 expression.

Methods

BAT Cell Density and Adipocyte Area

Mice:

C57BL/6J male and female breeding mice from The Jackson Laboratories (Stock# 00664) aged 8 weeks old were used to produce offspring. Mice were housed under standard conditions and chow fed ad libitum supplied by University of California, San Diego. Pregnancies began 3 months after arrival under standard conditions. Protocol approved by IACUC at the University of California, San Diego.

Embedding and Sectioning:

Performed Paraffin Embedded Formalin Fixation. C57BL/6J pups were sacrificed at E15.5, E16.5, E17.5, E18.5, P0.5, P2.5, P4.5, P8.5, P12.5, P20.5, and P30.5 while corresponding dams were sacrificed on E18.5. We excised iBAT at each time point. Tissues incubated in 10% (vol./vol.) Formalin Formal Fresh (Thermo Fisher Scientific; Lot# 140046) overnight at 4□, followed by a 70% ethanol incubation overnight at 4°C. Tissues were then dehydrated using 95% ethanol for 2 washes of 30 minutes on ice, then 100% ethanol for 3 washes of 30 minutes on ice. Xylene (Sigma-Aldrich; Lot# SHBH7313) was used to remove ethanol through 3 washes of 30 minutes at room temperature. Dabbing to remove excess xylene, tissues were placed into melted 60c paraffin wax (Paraplast Plus®; Sigma-Aldrich #P3863) for 3 washes of 30 minutes of incremental wax purity and encased in pure paraffin wax at room temperature. Slides were

sectioned at 5uM using a microtome onto Polysine® slides (Thermo Fisher Scientific; Cat# P4981-001) and stored at room temperature.

Hematoxylin and Eosin Staining:

A regressive stain at room temperature was accomplished for iBAT samples by first removing paraffin from slides using 2 washes of xylene for 3 minutes each. Slides were then hydrated using decreasing concentrations of ethanol at 1 wash for 30 seconds starting with 100%, then 95%, then 80% ethanol. 1 wash of DI water for 30 seconds fully hydrated the slides. Filtered Gill 3 Hematoxylin (Thermo Fisher Scientific; #72611) was used to stain nuclei for 1 min. 3 washes of DI water for 30 seconds removed excess Gill 3 Hematoxylin. Sections were then washed in 0.5% Acid Alcohol solution (1mL HCL, 199mL 70% Ethanol) for 10 seconds to regress Hematoxylin staining and lighten blue hues. 3 washes of DI water for 30 seconds removed excess 0.5% Acid Alcohol. This was followed by Scott's Tap Water Solution (2.0g sodium bicarbonate, 20g magnesium sulfate, fill to 1000mL with tap water) wash for 10 seconds to regain blue color to nuclei. 3 washes of Di water for 30 seconds removed excess Scott's Tap Water Solution. Eosin Y (Thermo Fisher Scientific; #E-511 Lot #905213) as 1% solution in 95% EtOH was used for 10 seconds to counterstain for cellular cytoplasm. Sections were then dehydrated using subsequent washes of increasing ethanol for 1 wash in 80% and 95% for 30 seconds, and 2 washes in 100% washes for 1 minute. 2 washes of xylene for 3 minutes removed excess alcohol. Sections were air dried and mounted using Toluene Solution hardening mounting medium (Thermo Fisher Scientific; Lot# 157602) overnight at room temperature.

Imaging:

iBAT sections were viewed on a Nikon Eclipse E800 microscope at 4x, 10x, 20x, and 40x magnifications under standard bright field light source. 8 distinct images of iBAT were taken at each magnification using a camera from RT SE from Diagnostic Instruments, Inc. (Serial# 228479) on default settings. SPOT Advanced™ v. 4.6 image software was used to analyze images on default brightfield application and saved as a Tagged Image File Format (TIFF) file.

Measuring Cell Density and Adipocyte Area:

Used ImageJ (64-bit Java 1.8.0_112) software to analyze cell density of iBAT at 40x magnification. Opened image files and darkened nuclei using "Color Balance". Split the image into 3-color channels using "Split Channels" and selected only the Red channel. Converted the Red channel to black and white and adjusted "Threshold" until nuclei stand out as black circles and remaining cellular structures disappear. Used the "Analyze Particles" function to count each nucleus. Used the "Measure" function to find the total area of the tissue. Divided the number of nuclei by the total area to get Cell Density. Averaged the data from 8 images per time point and generated a graph in Microsoft Excel 2016. Adipocyte area used the same image and protocol, except images were first inverted using the “Invert” function before converting to black and white. This allowed us to target the previously white spaces which indicated multilocular lipid droplets. The rest of the procedure remained unchanged.

Statistical Analysis:

Data expressed as mean ± standard deviations. Student's T-Test was used to determine p-values compared to E18.5. A p-value of <0.05 is considered significant.

BAT Mass Ratio

Mice:

C57BL/6J male and female breeding mice from The Jackson Laboratories (Stock# 00664) aged 8 weeks old were used to produce offspring. Mice were housed under standard conditions and chow fed ad libitum supplied by University of California, San Diego. Pregnancies began 3 months after arrival under standard conditions. Protocol approved by IACUC at the University of California, San Diego.

Mass Measurement:

9 pups were taken on each time point of E18.5, P0.5, P2.5, P3.5, P4.5, P8.5, P12.5, P20.5, P30.5, and P180.5 and weighed on a scale (APX-60; Denver Instrument) in grams. iBAT samples were surgically removed from each pup and independently weighed on the same scale in milligrams. iBAT to total body weight mass ratios were calculated and averaged per time point. Results were graphed in Microsoft Excel 2016.

Statistical Analysis:

Data expressed as mean ± standard error of the mean. Student's T-Test was used to determine p-values compared to E18.5. A p-value of <0.05 is considered significant.

Analysis of UCP1 Protein:

Mice:

C57BL/6J male and female breeding mice from The Jackson Laboratories (Stock# 00664) aged 8 weeks old were used to produce offspring. Mice were housed under standard conditions and chow fed ad libitum supplied by University of California, San Diego. Pregnancies began 3 months after arrival under standard conditions. Protocol approved by IACUC at the University of California, San Diego.

Tissue Lysis:

iBAT samples were surgically removed from pups on E15.5, E16.5, E17.5, E18.5, P0.5, P2.5, P4.5, P8.5, P14.5, P20.5, P22.5, P30.5 and placed onto dry ice in eppendorf tubes. Added 300uL lysis buffer (6g HEPES, 22.3g sodium phosphate, 2.1g sodium fluoride, 1.86g EDTA, 5mL Triton X100, DI water to bring volume to 500mL, pH 7.5) and vortexed to mix. Kept sample on ice and homogenized (Precellys® 24 Homogenizer; Bertin Technologies). Centrifuged samples at 4°C for 30 minutes at 13300 rpm (Labnet C2400-R MicroCentrifuge).

Protein Concentration:

Protein concentration was determined by adding 200uL of 1:5 dilution of Bradford Protein Assay (BIO-RAD; Cat# 500-0006) in DI water and 1uL of lysed tissue to an assay plate. Loaded protein standard in empty wells (BSA in DI water with dilution factors of 0.625, 1.25, 2.5, 5, 10, and 20). After shaking the assay plate to mix, we set the plate inside the plate reader (EPOCH BioTek Instruments, Inc.; Serial# 13030610). Analyzed protein concentration using Gen5 (v. 2.03) software from BioTek. Set final protein concentration to 30ug of iBAT and took note of the volume needed in each time point.

Western Blot:

We added 8uL loading buffer to lysed tissues (0.93g DTT, 1g SDS, 3mL glycerol) and set on a heat block at 70°C for 12 minutes. We spun down our samples and loaded them into 10% SDS-PAGE gels (9.7uL DI water, 5uL 40% acrylamide, 5uL 1.5M tris at pH 8.8, 200uL 10% SDS, 200uL 10% APS, 25uL TEMED; stacking gel 5.3uL DI water, 0.7uL 40% acrylamide, 1.14uL 1M tris at pH 6.8, 80uL 10% SDS, 80uL 10% APS, 20uL TEMED) in duplicate for each time point. We added 7.5uL protein ladder (Precision Plus Protein™; Bio-Rad Cat# 161-0374) into an empty well and ran the gel at 100V to align bands, then 125V until bands run to bottom (PowerPac Basic; BIO-RAD Serial# 041BR 16045). Labeled a PVDF membrane (Immuno-Blot®; BIO-RAD Cat# 162-0177) and allowed to soak in methanol for 1 minute, then in transfer buffer (50mL 20X NuPAGE® Transfer Buffer, 100mL methanol, DI water to 1L) for 20 minutes. Removed SDS-PAGE gel and stacked on top of PVDF membrane in cassette with sponges and filter paper. Placed into transfer rig (Mini PROTEAN® 3 Cell; BIO-RAD Serial#

525BR 064550) and ran at 100V for 90 minutes. Once transfer completed, we removed the PVDF membrane and placed into 5% milk blocking buffer (1g milk powder, 20mL 1x TBST) shaken for 1 hour at room temperature. After 2 washes of 1x TBST for 5 minutes each, we placed the membrane into rabbit anti-UCP1 primary antibody (Abcam; ab23841) at 1:10,000 concentration in antibody diluent (10uL antibody, 0.5g milk powder, 100uL 1% sodium azide, 10mL 1x TBST) shaken overnight at 4°C. After 2 washes of 1x TBST for 15 minutes each, we placed the membrane into mouse anti-rabbit IgG HRP secondary antibody (Santa Cruz Biotechnology; sc-2357) at 1:5000 concentration in milk blocking buffer shaken for 1 hour at room temperature. After 3 washes of 1x TBST for 15 minutes each, we applied 500uL of ECL solution (SuperSignal™; Thermo Fisher Scientific Prod# 34578) onto the membrane and allowed it to sit for 2 minutes before flipping the membrane upside down for 2 minutes to spread the ECL. We exposed the membrane for 1 minute on autoradiograph films (MidSci; Lot# 79660015) and uploaded a digital version of the image using a scanner (Epson Perfection 4870 Photo). Our loading control followed the same protocol using rabbit anti-GAPDH (Santa Cruz Technologies; sc-25778) at 1:10,000 concentration in antibody diluent and washed in mouse anti-rabbit IgG HRP secondary antibody at 1:5000 concentration in milk blocking buffer. We exposed GAPDH for 30 minutes on autoradiograph films.

Western Blot Quantification:

Quantified Western Blot results using Image Studio Lite (5.x) software. Followed the protocol provided by Li-Cor (Doc # 988-15592). Subtracted the "Background" measurement from the "Signal" measurement for each band. Normalized to GAPDH loading control by

dividing the corresponding measurement in UCP1 by GAPDH per band. Averaged each time point and graphed data on Microsoft excel 2016.

Statistical Analysis:

Data expressed as mean ± standard deviations. Student's T-Test was used to determine p-values compared to E18.5. A p-value of <0.05 is considered significant.

UCP1-creER mT/mG Analysis

Animal Models:

UCP1-creER male mouse breeder was supplied by Christian Wolfrum lab and arrived aged 8 weeks old (Rosenwald 2013). ROSA$^{mT/mG}$ (known as mT/mG) female mice came from The Jackson Laboratories (Stock# 007576) aged 8 weeks old. We crossbred these mice and their progeny until we achieved UCP1-creER mT/mG triple homozygous transgenic mice. Genotyped the UCP1-creER using QPCR mastermix (SsoAdvanced™; BIORAD #1725270) with Cre primers (The Jackson Laboratories; primer# 1083 cre, 1085 cre) as well as a probe.

Gavage:

Gavage using 100ul Tamoxifen solution (Sigma-Aldrich; T5648-1G) at 2mg Tamoxifen/100ul using sunflower oil. Administered via oral gavage each day from four days before time point sacrifice at noon at room temperature to pregnant dams.

Tissue Collection:

Dams anesthetized using ketamine anesthetic (500uL Ketamine, 250uL xylazine, 4.25mL Saline) via intraperitoneal injection. Perfused using cold 1x PBS with automated perfusion pump to drain blood. Collected iBAT and aBAT samples from dams and stored in 4% PFA overnight at 4°C on E17.5 and E18.5. Genotyped pups tails to ensure triple homozygous UCP1-creER mT/G genotype. Fixed whole pups in 4% PFA overnight at 4°C. All tissue collection was completed with minimal light to prevent photobleaching.

Optimal Cutting Temperature Embedding:

Sucrose infiltrated all samples for cryoprotection in 10% sucrose solution overnight at 4°C (50g D-Saccharose, 202.5mL 0.2M disodium phosphate, 47.5mL 0.2M sodium phosphate buffer, 250mL distilled water), then 30% sucrose solution overnight at 4°C (150g D-Saccharose, 202.5mL 0.2M disodium phosphate, 47.5mL 0.2M sodium phosphate buffer, 250mL distilled water). Blot dried samples and embedded in OCT Compound (Tissue-Plus®; Thermo Fisher Scientific). Flash frozen using dry ice in 2-methyl-butane (Sigma-Aldrich; Lot# SHBF6800V). Stored in -20°C until use. Dam iBAT and aBAT were sectioned in cryostat at -20°C at 5uM onto polysine slides. Whole pups were sectioned sagittally until iBAT and aBAT were visible under the same conditions. All embedding and sectioning was completed with minimal light to prevent photobleaching.

Staining:

Applied 100uL DAPI mounting medium (DAPI-Fluoromount-G®; SouthernBiotech Cat# 0100-20) directly onto air dried sections. Placed cover slip in top of samples and allowed to dry overnight at room temperature. All staining was completed with minimal light to prevent photobleaching.

Imaging:

Tissue sections were viewed on a Nikon Eclipse E800 microscope using a Mercury lamp for fluorescence at 4x, 10x, 20x, and 40x magnifications with DAPI, TRITC, FITC fluorescence filters. At least 8 distinct images of iBAT and aBAT were taken at each magnification at each time point. Used SPOT Advanced™ v. 4.6 image software to merge each color channel and saved the images as Tagged Image File Format (TIFF) files.

High Fat Fetal Programming

Animal Conditions:

C57BL/6J male and female breeding mice from The Jackson Laboratories (Stock# 00664) aged 8 weeks old were used to produce offspring. Female mice were housed under standard conditions and fed high fat diet consisting of 60% of caloric intake from fat (Research Diets, Inc. formula D12492) ad libitum 3 months before pregnancy. Protocol approved by IACUC at the University of California, San Diego.

Embedding and Sectioning:

Paraffin Embedded Formalin Fixed protocol as mentioned earlier. Sectioned whole pups at P0.5 and P10.5 time points. Sectioned at 5uM along sagittal plane until iBAT and aBAT were visible on microtome.

Immunohistochemistry Staining:

An immunohistochemistry stain was performed. We deparaffinized sections using xylene (Sigma-Aldrich; Lot# SHBH7313) for 3 washes of 5 min, then dehydrated them in decreasing ethanol washes of two times for 10 minutes in 100% , 95%, then DI water. Antigen retrieval was set in 0.1M citrate buffer (19.2g citric acid anhydrous, 4.5mL Tween 20, diH2O until 1 liter, pH 6.0) at 95°C for 30 minutes. An endogenous peroxide block was done using 2% hydrogen peroxide in water for 10 minutes. An endogenous biotin wash was done using Avidin and Biotin for 15 minutes each (Vector Laboratories, Inc.; SP-2001). An endogenous collagen block was done using rabbit blocking buffer (2% normal rabbit serum, 1% BSA, 0.02% sodium azide, 0.2% Triton-X100, 1x PBS until 250mL, pH to 7.4) for 1 hour at room temperature in damp conditions. Sections were incubated in primary antibody using anti-UCP1 antibody (Abcam; ab23841) at 1:200 in rabbit blocking buffer overnight at 4°C in damp conditions. The negative control was incubated in rabbit blocking buffer instead of primary antibody. Secondary antibody incubation was done using biotin labeled goat anti-rabbit IgG (KLP; Cat# 16-15-06) at 1:200 in rabbit blocking buffer for 1 hour room temperature in damp conditions. Our slides were then incubated in a tertiary reagent using ABC solution (Vectastain ABC Kit PK-6100; Vector Laboratories, Inc.) for 1 hour at room temperature in damp conditions. DAB staining was done

using 3 drops of DAB solution (ImmPACT DAB SK-4105; Vector Laboratories, Inc.) per slide for 3 minutes followed by an immersion in 1x PBST to halt the reaction. We counterstained our slides using 2 drops of 30% Gill 3 in water for 5 seconds. Then we dehydrated our slides in increasing ethanol washes from 70%, 95%, then 100% for 2 washes of 1 minute each. We washed our slides in xylene for 2 washes of 3 minutes each to remove excess alcohol. After air drying, we mounted our slides using Toluene Solution hardening mounting medium (Thermo Fisher Scientific; Lot# 157602)) and coverslip overnight at room temp. Between each step we washed sections our slides in 1x PBST for 3 washes of 5 minutes to clear away previous chemicals.

Imaging:

Tissue sections were viewed on a Nikon Eclipse E800 microscope at 4x, 10x, 20x, and 40x magnifications under standard bright field light source. At least 4 distinct images of iBAT were taken at each magnification using a camera on default settings. SPOT Advanced™ v. 4.6 image software was used to analyze images on default brightfield application and saved as a Tagged Image File Format (TIFF) file.

Results

Fetal BAT decreases in cell density postpartum

Adult brown adipocytes contain a single nucleus surrounded by multilocular lipid droplets and interspaced with specialized thermogenic mitochondria. Brown adipose tissue is adaptable, especially during perinatal development. We sought to identify the morphology of BAT at various time points including embryonic and postpartum time frames. Fetal mouse iBAT was obtained from embryonic day 18.5 (E18.5) to postpartum day 30.5 (P30.5). E18.5 iBAT is densely packed with nuclei and the cellular structure is amorphous with no cell walls to clearly define cells apart. (Fig. 1A). This pattern persists until P4.5, when the nuclei spread out and interstitial regions are now identifiable. iBAT nuclei remain clumped in certain regions as seen from P4.5 to P12.5. From P20.5 onward, cellular structure is distinctive, with iBAT nuclei pronounced and surrounded by a circular cellular structure. A comparison between E18.5 and P30.5 further highlights the morphological development iBAT undergoes (Fig. 1B). Maternal iBAT on E18.5 was taken as a frame of reference and shows similar nuclei disbursement and interstitial spread as P30.5 (Fig. 1A).

Quantifying the nuclei density in each time point with eight separate sections reveals a negative association between iBAT cell density and time (Fig. 1C). This was done using the ImageJ software to digitally count nuclei and assess the nuclei to tissue area ratio. As developmental time progresses, the density of iBAT nuclei generally decreases. P4.5 appears to have an even lower nuclei to tissue area ratio compared to the next time point at P8.5. However, compared to the E18.5 fetal BAT, each time point except for P0.5 shows a significant increase in

cell density. The nuclei remain the same size between each time point. Rather, the cells are expanding, as cytoplasmic space (uncolored) enlarges around a central nucleus.

Brown adipocytes in adult BAT have a multilocular disbursement of lipid droplets within the interstitial space. As such, we explored the morphology of lipid containing adipocytes (Fig. 1D). The lipid droplets appear as clear or white circular areas within the circular cellular structures due to washing out during embedding (Fig. 1A). Fetal iBAT from E18.5 through P2.5 lack clear multilocular structure as circular lipid droplets are not present. Starting from P4.5, the lipid droplets are identifiable as they appear circular. This pattern persists and is compounded by P30.5. As the graph shows, the percentage of total lipid droplet area increases with increasing developmental time point. Indeed, compared to E18.5 fetal iBAT, developmental time point P2.5 and onward show a significant increase in lipid droplet to tissue area ratio. Between P8.5 and P12.5, we see the largest increase in lipid droplet percent area. Following P12.5, the remaining time points plateau and approach that of Dam E18.5 iBAT.

BAT has been known to vary in mass in correspondence to age. We explored how BAT changes in mass at each time point. Using C57BL/6J dams under normal conditions, we surgically removed iBAT from nine pups at each time point and weighed them individually. Comparing the mass of iBAT with the total body weight of each pup, we were able to see how iBAT changes its relative mass through time. Results indicate a significant increase in relative iBAT mass from E18.5 to P0.5, with a general decrease after birth through to adolescence at P180.5 (Fig. 1E).

UCP1 is expressed during late embryonic stage

Uncoupling protein 1 (UCP1) is the key protein in brown adipocytes responsible for thermogenic capacity. We sought to identify the gestational time frame when UCP1 is expressed. Using C56BL/6 mice, we analyzed UCP1 protein expression at various time points from E15.5 to P30.5 (Fig. 2A). Quantifying the Western blots and normalizing to housekeeping gene GAPDH reveals these trends graphically, notably the apparent curve of UCP1 protein expression through time (Fig. 2B). The Western blot shows UCP1 protein detection beginning at E17.5. UCP1 protein levels in iBAT rapidly increased upon birth, with P0.5 and onward showing sustained elevated expression. After P20.5, UCP1 protein levels begin to decrease.

To further investigate whether the signal from the Western blot is accurate, we bred UCP1-creER mT/mG mice that express GFP upon activation of UCP1 promoter and RFP in the absence of activation. The mT/mG construct allows for native double fluorescence reporter proteins in transgenic mice. LoxP sites flank tandem dimer Tomato (mT) that uses a CMV enhancer to drive production. Downstream of these LoxP sites is the sequence for Enhanced GFP (mG) with a polyadenosine tail. Without activation of Cre-recombinase, membrane-targeted mT is expressed, producing red fluorescent proteins. After Cre recombinase excision of the LoxP sites, membrane-targeted mG is expressed producing green fluorescent proteins. UCP1-CreER is a Tamoxifen-inducible Cre-recombinase expressed by the UCP1 promoter. By recombining UCP1-CreER mice with mT/mG mice, we were able to produce UCP1-CreER mT/mG triple homozygous mice. As such, mT is expressed globally except when UCP1 is activated by its promoter. In this case, mG is produced instead. Green and red signals do not overlap, establishing a simple double fluorescent screen for UCP1 promoter driven expression. Using this construct, we aimed to examine UCP1 activity on a cellular level. iBAT sections were taken

from both fetal E18.5 pups and dam E18.5 mothers (Fig. 2C). Results indicate positive green signals very clearly in dam E18.5 iBAT. More interestingly, fetal E18.5 iBAT also expresses positive green signals though they appear faintly. Fetal E17.5 iBAT did not show significant signals (data not shown). These results indicate UCP1 expression occurs during late gestation in mice pups, with emphasis on E18.5 showcasing a visual representation.

High fat maternal diet increases UCP1 expression in neonate pups

Maternal obesity during gestation has been shown to foreshadow numerous health complications for offspring during adolescence (Sullivan 2015). We investigated the effect of maternal obesity on fetal BAT development and UCP1 expression. Maternal obesity was created by feeding C57BL/6 female mice 3 months on high-fat (HF) diet where 60% calories were from fat. Control dams were fed with regular chow (RD). We analyzed the iBAT of neonates on P0.5. Using immunohistochemistry approach with anti-UCP1 antibody, we were able to localize and identify the presence of UCP1 protein in whole body sections of these neonates. Results show that iBAT under HF dam conditions show an increase in UCP1 protein expression compared to RD dam conditions (Figs. 3A and 3B). A stain without primary anti-UCP1 antibody serves to act as the negative control to control for endogenous signals (Fig. 3C). This may suggest iBAT is readily influenced by maternal obesity and plays a larger role in thermogenic activity on P0.5.

Discussion

Brown adipose tissue is a versatile component of mammalian physiology that produces heat. Studies have focused on its thermogenic qualities, pathway of activation, and nascent therapeutic capabilities (Klingenspor 2017, Enerbäck 2010, Chechi 2013). While there is still much to gain in these fields, there lacks information on BAT development and the effect of maternal obesity on BAT development. Investigation into this process facilitates a greater understanding of BAT physiology in a pediatric setting that may serve in the development of robust therapies aimed at offsetting the deleterious effects of obesity.

In this study, we examined the morphology of BAT at various developmental stages, including both embryonic and postpartum time frames. Our goal was to describe how BAT develops in terms of its tissue mass, morphology, and UCP1 expression. There are two ways to study iBAT mass: absolute tissue mass and iBAT/body weight ratio. Although there is a significant increase in iBAT absolute mass, the iBAT/BW ratio represents the dynamic nature of BAT development during perinatal period. iBAT mass to body weight ratios reveals a significant increase at birth on P0.5 as well as a significant decrease at adolescence on P180.5 compared to E18.5. This may indicate a shift in the relevancy of BAT at different developmental stages in offspring, namely that BAT seems to play a more significant thermoregulatory role at birth than through adolescence. As mice are altricial species and are unable to fend for themselves at birth, having an increased mass ratio of BAT may thermogenically protect against potential adverse cold environments.

We then investigated the morphology of the tissue. By using hematoxylin and eosin stained BAT samples at distinguished time points from C57BL/6J wild type mouse pups and

dam, we were able to visualize a decrease in adipocyte cell density as developmental time progressed. Likely, this decrease in cell density was brought on by an increase in lipid deposits within each cell. The cellular structure of brown adipocytes in human adults is comprised of multilocular lipid droplets surrounded by mitochondria, with the nucleus pushed to near the cell wall (Albright 1998). Indeed, these multilocular lipid droplets have been shown to increase in size during embryonic development. C57BL/6 mice pups from E15.5 through P0.5 show increased multilocular lipid droplet area and structural development within classical BAT deposits (Schulz 2013). Our results continue to highlight this increase in multilocular lipid droplet size through P30.5, showcasing the developmental progression of lipid accumulation during the postpartum time frame.

Additionally, our study examined the expression of UCP1 protein in C57BL/6J wild type mice pups. By using Western blotting, we were able to measure the UCP1 protein directly. Our results indicate UCP1 protein is produced as early as E17.5 and sets the stage for the timeline of embryonic expression of UCP1. We observed a dramatic increase in UCP1 protein expression beginning at P0.5 compared to embryonic time points, but noticed it tapered off before P20.5. We speculate the initial increase in UCP1 protein suggests necessity for heat production during the early time frame of postpartum neonates, while the decrease in UCP1 protein implies a reduced need later in life. To supplement our findings, we explored native UCP1 gene activity through the transgenic UCP1-creERmT/mG construct. Identifying iBAT UCP1 gene activity in E18.5 fetal pups provides an alternative method to representing our data. Interestingly, we were unable to properly visualize UCP1 gene activity in E17.5 pups even though we found UCP1 protein production at this time point. This may be due to excessive background interference from autofluorescence masking positive signals, as positive signals may be too weak. Regardless, we

successfully demonstrated that the UCP1-creER mT/mG transgenic construct can visualize UCP1 gene activity in embryonic pups. This serves to further validate the developmental time frame of UCP1 and sets up UCP1-creER mT/mG transgenic mice as a viable model in embryonic studies.

Interestingly, while we noticed a significant increase in UCP1 expression on P0.5 compared to E18.5, we did not find a significant difference in lipid accumulation on these time points. We speculate the reason why there is no significant change in lipid accumulation on P0.5 is because the recently birthed pups have not yet begun to nurse. They lack substantial fats provided through nursing and this is reflected in the low levels of lipid accumulation in BAT seen at birth. By P2.5, the pups have already begun nursing, which may explain the rapid accumulation of lipids from then on. With UCP1 however, we speculate that the significant increase is related to the evolutionary need for thermogenic homeostasis at birth. With increased UCP1 expression, the pup can produce heat through non-shivering thermogenesis and survive cold environments. However, to produce heat UCP1 requires activation by long chain fatty acids (Fedorenko 2013). The relationship between high UCP1 expression and low lipid accumulation at P0.5 remains to be clarified.

Obesity during pregnancy has been shown to increase the likelihood of hypertension, cardiovascular disease, and diabetes in offspring (Neri 2015). Following our investigation into how BAT develops during embryonic and postpartum stages of normal pregnancies, we also investigated the effects of maternal high fat diet on the expression of UCP1 in mice pups postpartum. By using immunohistochemistry staining for anti-UCP1 protein, we found that iBAT showed an increase in UCP1 expression on P0.5. It is known that high fat diet stimulates UCP1 expression in mice. High fat diets with 30% to 82% of total calories from fat have been

shown to increase UCP1 mRNA and protein levels and in adult mice under 6 months (Fromme 2011). There is also evidence that maternal nutrition affects fetal brown adipocytes. Pregnant ewes fed high fat diets during the last third of their pregnancies developed a greater abundance of UCP1 and subsequently higher thermogenic activity compared to the offspring of control diet fed ewes (Budge 2000). We speculate based on the increase in UCP1 protein expression from iBAT on P0.5 that this tissue plays a protective role against a high fat fetal environment. This may overall stimulate dietary-induced thermogenesis to protect against hyperlipidemia caused by a high fat fetal environment in the pups, as an increase in serum triglycerides past a certain homeostatic set point triggers metabolic processes to counteract excessive diets (Lowell 2003). This may suggest iBAT plays a significant role at birth under high fat maternal conditions.

The nature of our study design was intended to be an exploration into the development of brown adipocytes in mice during both embryonic and postpartum time frames, as well as the effects of high fat maternal diet on fetal programming. However, it is important to note the limitations of our study. We used C57BL/6J mouse models for each of our experiments. Mouse models are often analogous to human physiology and in our case both species possess active iBAT (Sacks 2013). However, humans are precocial while mice are altricial. This difference is notably distinct during neonatal development, especially in brown adipocyte thermogenic output and UCP1 expression (Symonds 2015). As such, our mouse models cannot be used as a perfect representation for human systems. We measured the lipid deposit area indirectly instead of direct staining for BAT multilocular lipids. Due to the formalin-fixed paraffin embedding of BAT, stains specific for lipids like Oil Red O could not be physically implemented as the ethanol washes required dissolve lipids. As a result, our indirect measurement should only be used as an estimate for the presence of lipids in brown adipocytes. For the Western blots, UCP1-creER

mT/mG visualization, and immunohistochemistry for anti-UCP1 in neonates the sample size of mice pups used was small, as only 3-4 pups were viable. This may contribute to unrepresentative data that may skew our results.

We would like to follow up our study by investigating how maternal obesity affects BAT morphology and UCP1 production in both perinatal development and adulthood. Our experiment focused on the natural development of mouse brown adipocytes during embryonic and postpartum time frames, with an additional study examining the difference in UCP1 at birth due to maternal obesity. However, it is of great interest to expand our study to see the effect maternal obesity has on metabolism in pups during adulthood. Maternal obesity in humans has been shown to bring up children with an increased risk of obesity, cardiovascular disease, and diabetes within adolescence (Leddy 2008). By investigating the role BAT plays in dietary-induced thermogenesis, specifically to determine the extent UCP1 serves to protect against maladaptive fetal programming, we may reveal potential therapeutic strategies capable of combating obesity driven diseases.

In conclusion, our results highlight the morphology of brown adipocytes during embryonic and postpartum development and illustrate an increase in multilocular lipid deposition. Additionally, we were able to use the UCP1-creER mT/mG transgenic construct to fluorescently visualize UCP1 gene activity in fetal embryonic mice pups. We show that UCP1 expression increases under high fat maternal diet. Together, these findings provide fundamental knowledge on the development of BAT under standard and obese pregnancies.

Figures

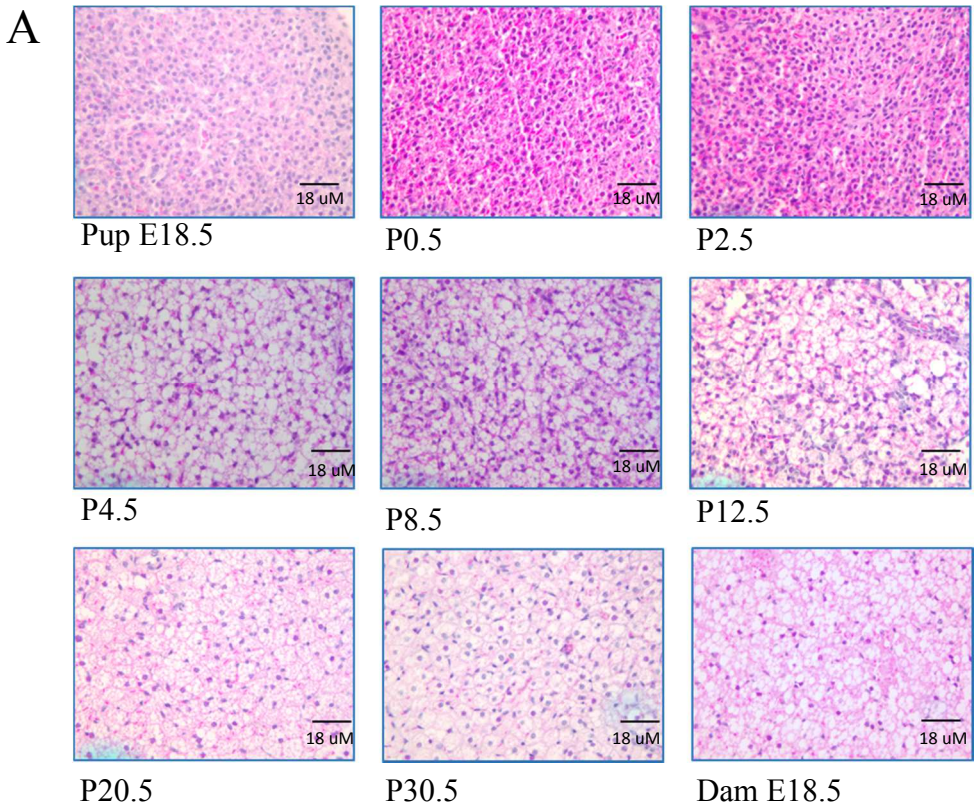

Figure 1. Gestation Affects Pup BAT Morphology by Decreasing Cell Density and Increasing Adiposity

A. Wild type mice pups iBAT harvested on E18.5, P0.5, P2.5, P4.5, P8.5, P12.5, P20.5, P30.5 along with Dam E18.5 iBAT. Sections were fixed in 10% formalin overnight, paraffin embedded, and cut at 5uM. Hematoxylin and Eosin staining preformed concurrently in a single setting. Magnification at 40x with scale bar shown.
B. Pup E18.5 and P30.5 selections from Figure. 1A enlarged to highlight hitological differences. Magnification at 40x with scale bar shown.
C. Cell density measurements using 8 distinct images from each time point. Standard deviations used as error bars. Student's T-Test used to determine significance when compared to Pup E18.5 data: ** = $p<0.01$.
D. Lipid droplet measurement as a percentage of total iBAT area using 8 distinct images from each time point. Standard deviations used as error bars. Student's T-Test used to determine significance when compared to Pup E18.5 data: ** = $p<0.01$.
E. iBAT mass compared to total body weight (BW) from 9 pups at each time point. SEM used as error bars. Student's T-Test used to determine significance when compared to Pup E18.5 data: * = $p<0.05$.

B

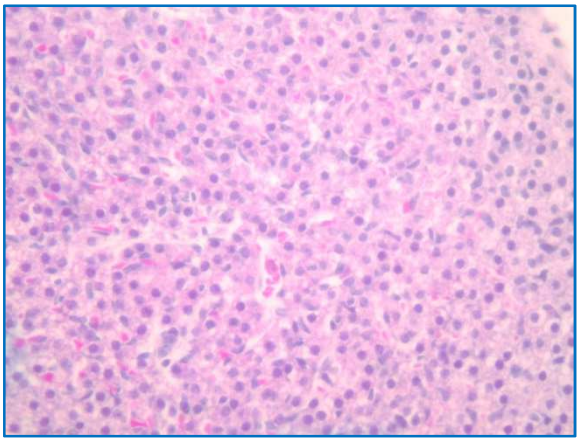

Pup E18.5

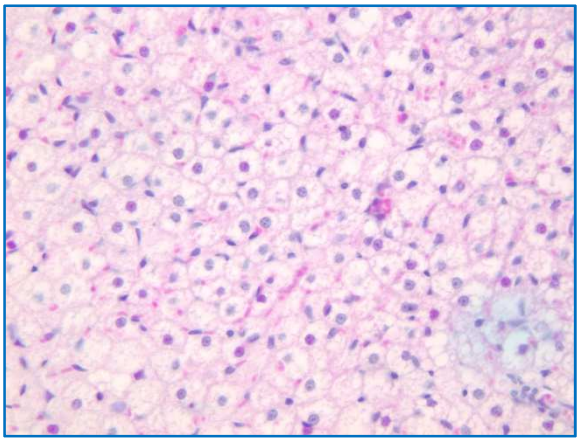

P30.5

Figure 1. continued

C

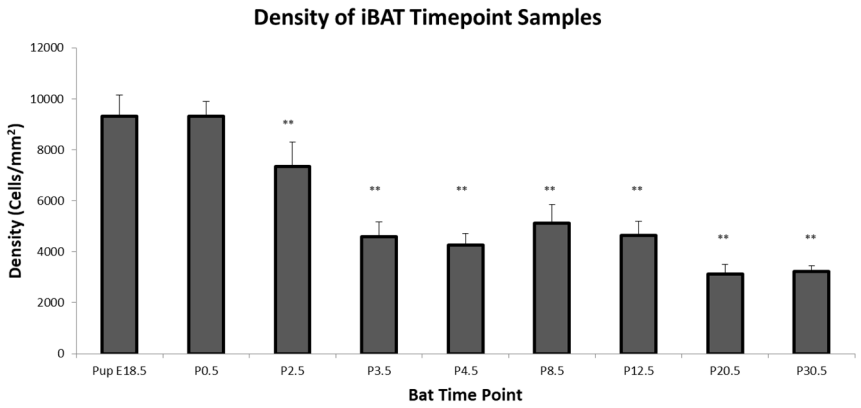

D

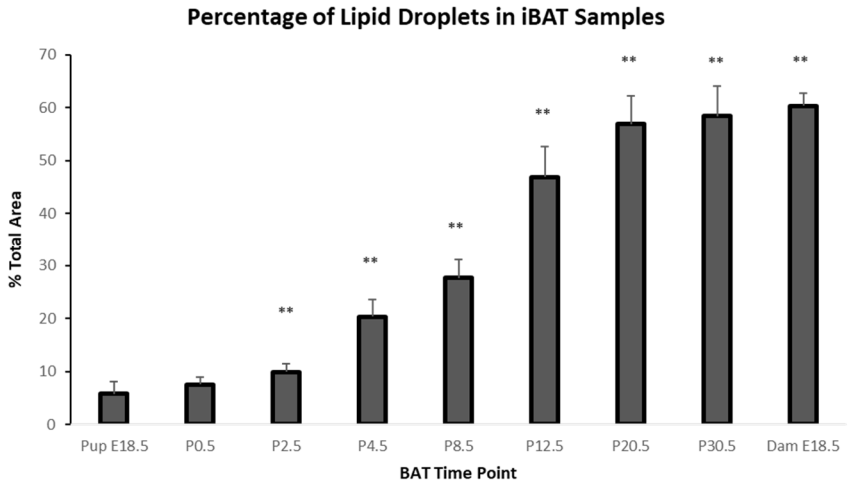

E

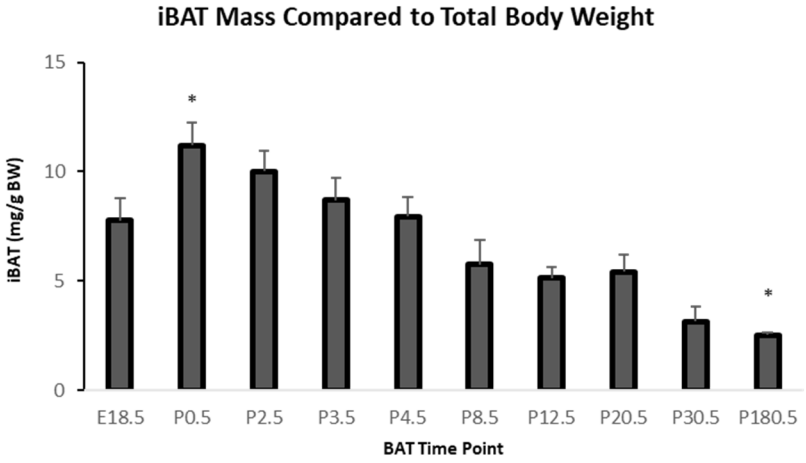

Figure 1. continued

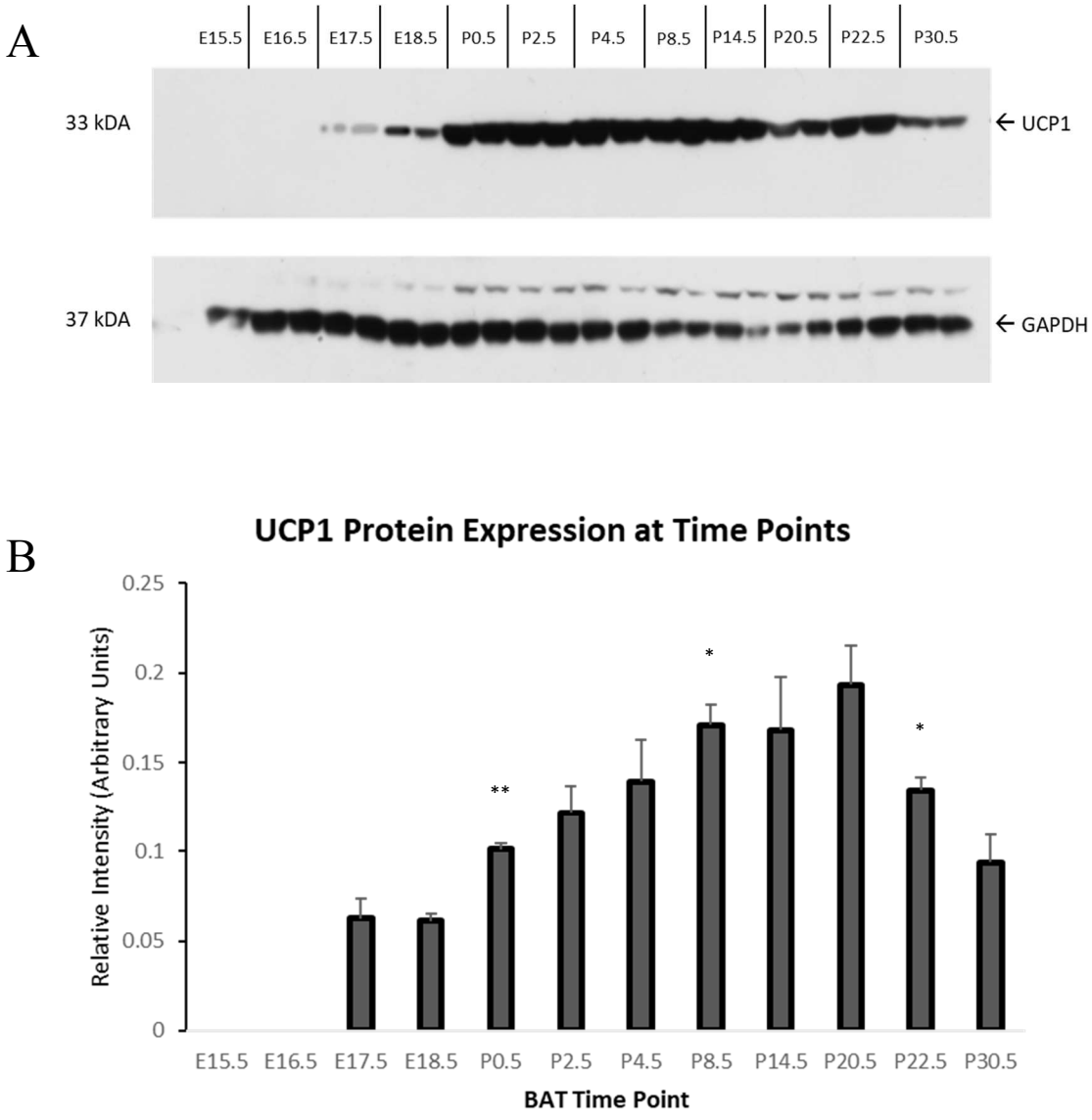

Figure 2. Visualization of UCP1 in Pup and Dam BAT at E18.5

A. Western result for anti-UCP1 antibody at E15.5, E16.5, E17.5, E18.5, P0.5, P2.5, P4.5, P8.5, P14.5, P20.5, P22.5 and P30.5. GAPDH measured as loading control.
B. Quantification of UCP1 results shown in Fig. 2A. Relative intensity as compared with GAPDH in arbitrary units. Student's T-Test used to determine significance when compared to Pup E18.5 data: * = $p<0.05$; ** = $p<0.01$.
C. UCP1-creER mT/mG iBAT from Pup (left) and Dam (right) were fixed in 4% PFA on E18.5 and embedded in OCT. Sections cut at 5uM and images taken using fluorescent microscope. Select positive signals circled in orange. Magnification is 20x with scale bar shown

C

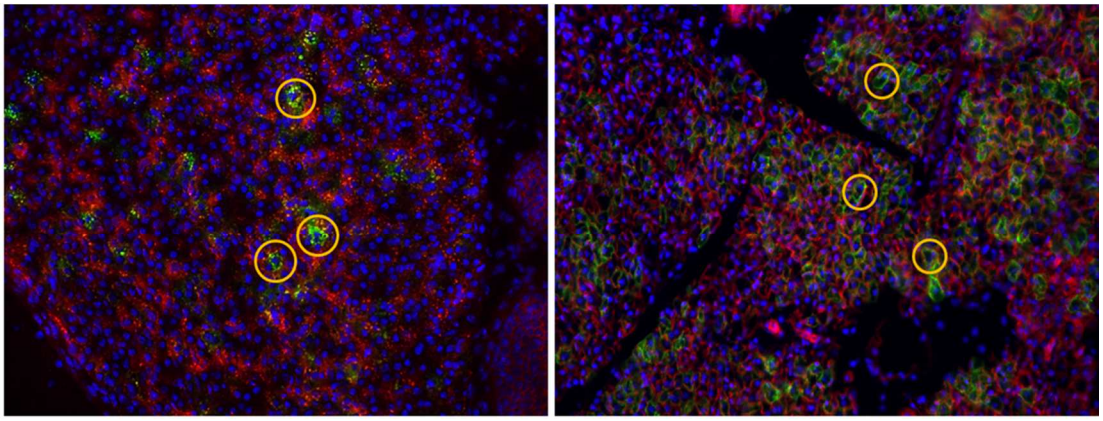

Pup E18.5 iBAT

Dam E18.5 iBAT

Figure 2. continued

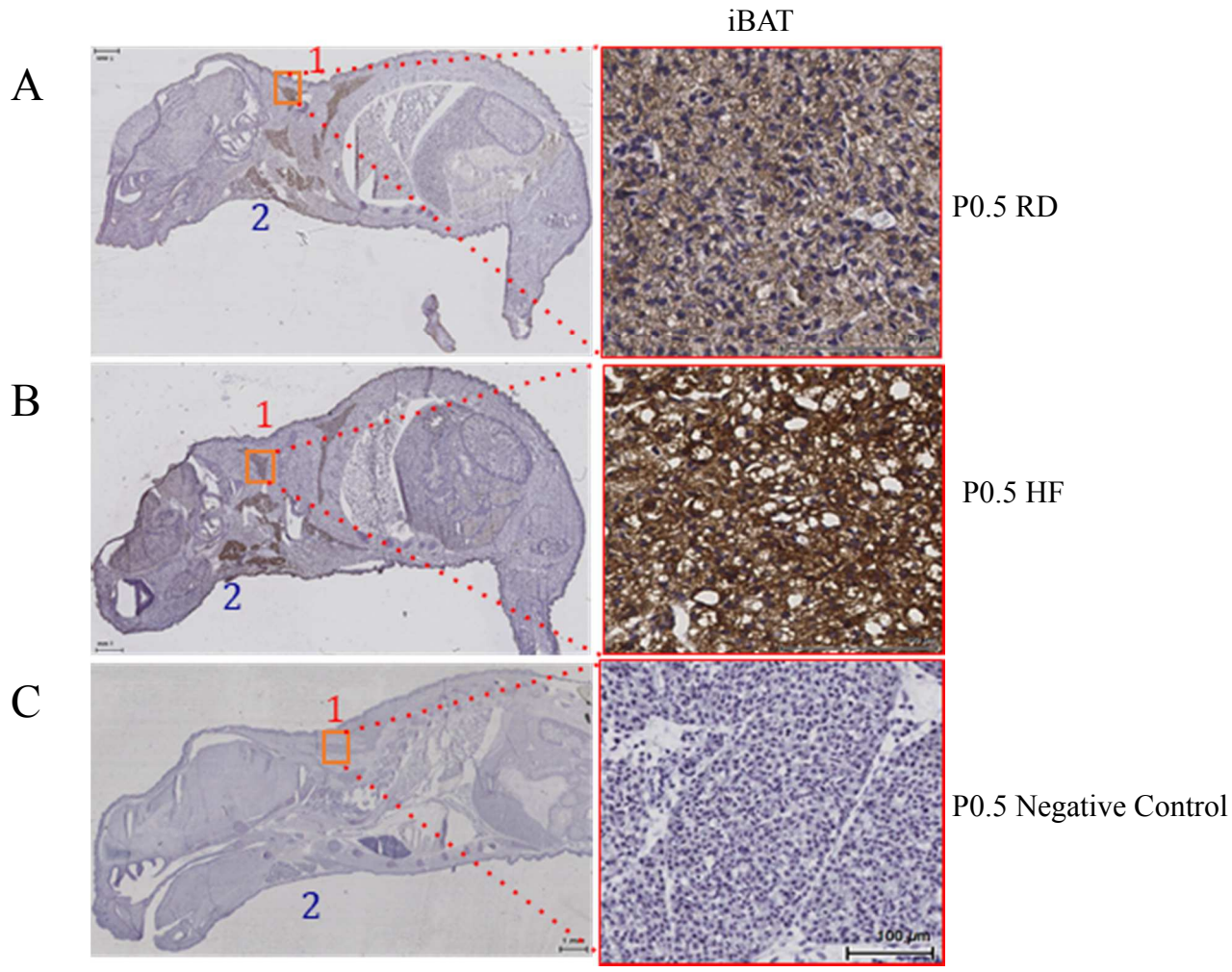

Figure 3. Maternal Obesity Affects UCP1 Expression in Infants

A. 5uM section of whole paraffin embedded pup at P0.5 under regular diet Dam condition (RD). iBAT shown. Staining done using anti-UCP1 IHC with DAB. Magnification at 10x with scale bar shown.
B. High fat fed Dam pups (HF) at P0.5. Embedding and staining conditions kept the same as Fig. 3A. Magnification at 10x with scale bar shown.
C. Negative control RD pup at P0.5. IHC done using blocking buffer instead of anti-UCP1 antibody. Magnification at 10x with scale bar shown.

References

Albright, A.L. and Stern, J.S. (1998). Adipose tissue. In: Encyclopedia of Sports Medicine and Science, T.D.Fahey (Editor). Internet Society for Sport Science: http://sportsci.org. 30 May 1998.

Allott, E. H., & Hursting, S. D. (2015). Obesity and cancer: Mechanistic insights from transdisciplinary studies. *Endocrine-Related Cancer,22*(6). doi:10.1530/erc-15-0400

Anouk A. J. J. Van Der Lans, Wierts, R., Vosselman, M. J., Schrauwen, P., Brans, B., & Lichtenbelt, W. D. (2014). Cold-activated brown adipose tissue in human adults: Methodological issues. *American Journal of Physiology-Regulatory, Integrative and Comparative Physiology,307*(2). doi:10.1152/ajpregu.00021.2014

Ashwal, E., & Hod, M. (2015). Gestational diabetes mellitus: Where are we now? *Clinica Chimica Acta,451*, 14-20. doi:10.1016/j.cca.2015.01.021

Bastien, M., Poirier, P., Lemieux, I., & Després, J. (2014). Overview of Epidemiology and Contribution of Obesity to Cardiovascular Disease. *Progress in Cardiovascular Diseases,56*(4), 369-381. doi:10.1016/j.pcad.2013.10.016

Boden, G. (2011). Obesity, insulin resistance and free fatty acids. *Current Opinion in Endocrinology, Diabetes and Obesity,18*(2), 139-143. doi:10.1097/med.0b013e3283444b09

Budge, H. (2002). The effect of maternal prolactin infusion during pregnancy on fetal adipose tissue development. *Journal of Endocrinology,174*(3), 427-433. doi:10.1677/joe.0.1740427

Budge, H., Bispham, J., Dandrea, J., Evans, E., Heasman, L., Ingleton, P. M., Evens, E., Sullivan, C., Wilson, V., Stephenson, T., Symonds, M. E. (2000). Effect of Maternal Nutrition on Brown Adipose Tissue and Its Prolactin Receptor Status in the Fetal Lamb. *Pediatric Research,47*(6), 781-786. doi:10.1203/00006450-200006000-00017

Cannon, B., & Nedergaard, J. (2004). Brown Adipose Tissue: Function and Physiological Significance. *Physiological Reviews,84*(1), 277-359. doi:10.1152/physrev.00015.2003

Chabowska-Kita, A., & Kozak, L. P. (2016). The critical period for brown adipocyte development: Genetic and environmental influences. *Obesity,24*(2), 283-290. doi:10.1002/oby.21376

Chechi, K., Nedergaard, J., & Richard, D. (2013). Brown adipose tissue as an anti-obesity tissue in humans. *Obesity Reviews,15*(2), 92-106. doi:10.1111/obr.12116

Chen, K. Y., Brychta, R. J., Linderman, J. D., Smith, S., Courville, A., Dieckmann, W., Herscovitch, P., Millo, C. M., Remaley, A., Lee, P., Celi, F. S. (2013). Brown Fat Activation Mediates Cold-Induced Thermogenesis in Adult Humans in Response to a Mild Decrease in Ambient Temperature. *The Journal of Clinical Endocrinology & Metabolism,98*(7). doi:10.1210/jc.2012-4213

Clarke, L., Bryant, M. J., Lomax, M. A., & Symonds, M. E. (1997). Maternal manipulation of brown adipose tissue and liver development in the ovine fetus during late gestation. *British Journal of Nutrition,77*(06), 871. doi:10.1079/bjn19970086

Cnop, M., Welsh, N., Jonas, J., Jorns, A., Lenzen, S., & Eizirik, D. L. (2005). Mechanisms of Pancreatic -Cell Death in Type 1 and Type 2 Diabetes: Many Differences, Few Similarities. *Diabetes,54*(Supplement 2). doi:10.2337/diabetes.54.suppl_2.s97

Copeland, K. C., Becker, D., Gottschalk, M., & Hale, D. (2005). Type 2 Diabetes in Children and Adolescents: Risk Factors, Diagnosis, and Treatment. *Clinical Diabetes,23*(4), 181-185. doi:10.2337/diaclin.23.4.181

Cypess, A. M., Lehman, S., Williams, G., Tal, I., Rodman, D., Goldfine, A. B., Kuo, F. C., Palmer, E. L., Tseng, Y., Doria, A., Kolodny, G. M., Kahn, C. R. (2009). Identification and Importance of Brown Adipose Tissue in Adult Humans. *New England Journal of Medicine,360*(15), 1509-1517. doi:10.1056/nejmoa0810780

Dunger, D. B., Ahmed, M. L., & Ong, K. K. (2005). Effects of obesity on growth and puberty. *Best Practice & Research Clinical Endocrinology & Metabolism,19*(3), 375-390. doi:10.1016/j.beem.2005.04.005

Ebbeling, C. B., Pawlak, D. B., & Ludwig, D. S. (2002). Childhood obesity: Public-health crisis, common sense cure. *The Lancet,360*(9331), 473-482. doi:10.1016/s0140-6736(02)09678-2

Egger, G., & Dixon, J. (2014). Beyond Obesity and Lifestyle: A Review of 21st Century Chronic Disease Determinants. *BioMed Research International,2014*, 1-12. doi:10.1155/2014/731685

Enerbäck, S. (2010). Brown adipose tissue in humans. *International Journal of Obesity,34*(S1). doi:10.1038/ijo.2010.183

Fasshauer, M., Blüher, M., & Stumvoll, M. (2014). Adipokines in gestational diabetes. *The Lancet Diabetes & Endocrinology,2*(6), 488-499. doi:10.1016/s2213-8587(13)70176-1

Fedorenko, A., Lishko, P. V., & Kirichok, Y. (2012). Mechanism of Fatty-Acid-Dependent UCP1 Uncoupling in Brown Fat Mitochondria. Cell, 151(2), 400–413. doi.org/10.1016/j.cell.2012.09.010

Feldmann, H. M., Golozoubova, V., Cannon, B., & Nedergaard, J. (2009). UCP1 Ablation Induces Obesity and Abolishes Diet-Induced Thermogenesis in Mice Exempt from Thermal

Stress by Living at Thermoneutrality. *Cell Metabolism,9*(2), 203-209. doi:10.1016/j.cmet.2008.12.014

Finkelstein, E., Khavjou, O., Thompson, H., Trogdon, J., Sherry, B., & Dietz, W. (2012). Obesity and Severe Obesity Forecasts Through 2030. *American Journal of Preventive Medicine,42*(6). doi:10.1016/s0749-3797(12)00266-8

Finkelstein, E. A., Trogdon, J. G., Cohen, J. W., & Dietz, W. (2009). Annual Medical Spending Attributable To Obesity: Payer-And Service-Specific Estimates. *Health Affairs,28*(5). doi:10.1377/hlthaff.28.5.w822

Finkelstein, E. A., & Strombotne, K. L. (2010). The economics of obesity. *The American Journal of Clinical Nutrition,91*(5). doi:10.3945/ajcn.2010.28701e

Fromme, T., & Klingenspor, M. (2011). Uncoupling protein 1 expression and high-fat diets. *American Journal of Physiology-Regulatory, Integrative and Comparative Physiology,300*(1). doi:10.1152/ajpregu.00411.2010

Gammone, M., & Dorazio, N. (2015). Anti-Obesity Activity of the Marine Carotenoid Fucoxanthin. *Marine Drugs,13*(4), 2196-2214. doi:10.3390/md13042196

Genkinger, J. M., Kitahara, C. M., Bernstein, L., Gonzalez, A. B., Brotzman, M., Elena, J. W., Giles. G. G., Gartge, P., Singh P. N., Stolzengurg-Solomon R. Z., Weiderpass , E., Adami, H., O., Anderson, K.E., Beane-Freeman, L. E., Buring, J. E., Fraser, G. E., Fuchs, C. S., Gapstur, S. M., Gaziano, J. M., Helzlsouer, K. J., Lacey, J. V. Jr., Linet, M. S., Liu, J. J., Park, Y., Peters, U., Purdue, M. P., Robien, K., Schairer, C., Sesso, H. D., Visvanathan, K., White, E., Wolk, A., Wolpin, B. M., Zelenuich-Jacquotte, A., Jacobs, E. J. (2015). Central adiposity, obesity during early adulthood, and pancreatic cancer mortality in a pooled analysis of cohort studies. *Annals of Oncology,26*(11), 2257-2266. doi:10.1093/annonc/mdv355

Gesta, S., Tseng, Y., & Kahn, C. R. (2007). Developmental Origin of Fat: Tracking Obesity to Its Source. *Cell,131*(2), 242-256. doi:10.1016/j.cell.2007.10.004

Gestational Diabetes Mellitus. (2003). *Diabetes Care, 27* (Supplement 1). doi:10.2337/diacare.27.2007.s88

Hanson, C., Rutten, E., Wouters, E., & Rennard, S. (2014). Influence of diet and obesity on COPD development and outcomes. *International Journal of Chronic Obstructive Pulmonary Disease,*723. doi:10.2147/copd.s50111

Hassan, M., Latif, N., & Yacoub, M. (2012). Adipose tissue: Friend or foe? *Nature Reviews Cardiology,9*(12), 689-702. doi:10.1038/nrcardio.2012.148

Hibi, M., Oishi, S., Matsushita, M., Yoneshiro, T., Yamaguchi, T., Usui, C., Yasunaga, K., Katsuragi, Y., Kubota, K., Takana, S., Saito, M. (2016). Brown adipose tissue is involved in

diet-induced thermogenesis and whole-body fat utilization in healthy humans. *International Journal of Obesity,40*(11), 1655-1661. doi:10.1038/ijo.2016.124

Hill, M.A. (2018, July 16) Embryology *Mouse Timeline Detailed*. Retrieved from https://embryology.med.unsw.edu.au/embryology/index.php/Mouse_Timeline_Detailed

Kaufmans Atlas of Mouse Development Supplement. (2016). doi:10.1016/c2013-0-12676-1

Kearney, P. M., Whelton, M., Reynolds, K., Muntner, P., Whelton, P. K., & He, J. (2005). Global burden of hypertension: Analysis of worldwide data. *The Lancet,365*(9455), 217-223. doi:10.1016/s0140-6736(05)17741-1

Kelly, T., Yang, W., Chen, C., Reynolds, K., & He, J. (2008). Global burden of obesity in 2005 and projections to 2030. *International Journal of Obesity,32*(9), 1431-1437. doi:10.1038/ijo.2008.102

Klingenspor, M., Bast, A., Bolze, F., Li, Y., Maurer, S., Schweizer, S., Willershäuser, M., Fromme, T. (2017). Brown Adipose Tissue. *Adipose Tissue Biology,*91-147. doi:10.1007/978-3-319-52031-5_4

Kozak, L. P. (2010). Brown Fat and the Myth of Diet-Induced Thermogenesis. *Cell Metabolism,11*(4), 263-267. doi:10.1016/j.cmet.2010.03.009

Leddy, M. A., Power, M. L., & Schulkin, J. (2008). The Impact of Maternal Obesity on Maternal and Fetal Health. *Reviews in Obstetrics and Gynecology*, *1*(4), 170–178.

Lepper, C., & Fan, C. (2010). Inducible lineage tracing of Pax7-descendant cells reveals embryonic origin of adult satellite cells. *Genesis,48*(7), 424-436. doi:10.1002/dvg.20630

Lidell, M. E., Betz, M. J., & Enerbäck, S. (2014). Brown adipose tissue and its therapeutic potential. *Journal of Internal Medicine,276*(4), 364-377. doi:10.1111/joim.12255

Lin, J., Wu, P., Tarr, P. T., Lindenberg, K. S., St-Pierre, J., Zhang, C., Mootha, V. K., Jäger, S., Vianna, C. R., Reznick R. M., Cui, L., Maniera, M., Donovan, M. X., Wu, Z., Cooper M. P., Fan, M. C., Rohas, L. M., Zavacki, A. M., Cinti, S., Shulman, G. I., Lowell, B. B., Krainc, D., Spiegelman, B. M. (2004). Defects in Adaptive Energy Metabolism with CNS-Linked Hyperactivity in PGC-1α Null Mice. *Cell,119*(1), 121-135. doi:10.1016/j.cell.2004.09.013

Lowell, B. B., & Bachman, E. S. (2003). β-Adrenergic Receptors, Diet-induced Thermogenesis, and Obesity. *Journal of Biological Chemistry,278*(32), 29385-29388. doi:10.1074/jbc.r300011200

Metzger, B. E., Buchanan, T. A., Coustan, D. R., Leiva, A. D., Dunger, D. B., Hadden, D. R., . . . Zoupas, C. (2007). Summary and Recommendations of the Fifth International Workshop-

Conference on Gestational Diabetes Mellitus. *Diabetes Care,30*(Supplement 2). doi:10.2337/dc07-s225

Nakamura, K., Fuster, J. J., & Walsh, K. (2014). Adipokines: A link between obesity and cardiovascular disease. *Journal of Cardiology,63*(4), 250-259. doi:10.1016/j.jjcc.2013.11.006

Nedergaard, J., Golozoubova, V., Matthias, A., Asadi, A., Jacobsson, A., & Cannon, B. (2001). UCP1: The only protein able to mediate adaptive non-shivering thermogenesis and metabolic inefficiency. *Biochimica Et Biophysica Acta (BBA) - Bioenergetics,1504*(1), 82-106. doi:10.1016/s0005-2728(00)00247-4

Neri, C., & Edlow, A. G. (2015). Effects of Maternal Obesity on Fetal Programming: Molecular Approaches. *Cold Spring Harbor Perspectives in Medicine,6*(2). doi:10.1101/cshperspect.a026591

Neuhouser, M. L., Aragaki, A. K., Prentice, R. L., Manson, J. E., Chlebowski, R., Carty, C. L., . . . Anderson, G. L. (2015). Overweight, Obesity, and Postmenopausal Invasive Breast Cancer Risk. *JAMA Oncology,1*(5), 611. doi:10.1001/jamaoncol.2015.1546

Newkirk, K. D., Silverman, D. A., & Wynne-Edwards, K. E. (1995). Ontogeny of thermoregulation in the Djungarian hamster (Phodopus campbelli). *Physiology & Behavior,57*(1), 117-124. doi:10.1016/0031-9384(94)00220-y

Oelkrug, R., Polymeropoulos, E. T., & Jastroch, M. (2015). Brown adipose tissue: Physiological function and evolutionary significance. *Journal of Comparative Physiology B,185*(6), 587-606. doi:10.1007/s00360-015-0907-7

Ogden, C. L., Carroll, M. D., Fryar, C. D., & Flegal, K. M. (2015). Prevalence of Obesity Among Adults and Youth: United States, 2011–2014. *National Center for Health Sciences,209*.

Ogden C. L., Carroll, M. D., Kit B. K., Flegal K. M. (2014). Prevalence of Childhood and Adult Obesity in the United States, 2011-2012. *JAMA.* 2014;311(8):806–814. doi:10.1001/jama.2014.732

Park, J., Morley, T. S., Kim, M., Clegg, D. J., & Scherer, P. E. (2014). Obesity and cancer—mechanisms underlying tumour progression and recurrence. *Nature Reviews Endocrinology,10*(8), 455-465. doi:10.1038/nrendo.2014.94

Pope, M., Budge, H., & Symonds, M. E. (2013). The developmental transition of ovine adipose tissue through early life. *Acta Physiologica,210*(1), 20-30. doi:10.1111/apha.12053

Popkin, B. M., Adair, L. S., & Ng, S. W. (2012). Global nutrition transition and the pandemic of obesity in developing countries. *Nutrition Reviews,70*(1), 3-21. doi:10.1111/j.1753-4887.2011.00456.x

Rafael, J., & Wrabetz, E. (1976). Brown Adipose Tissue Mitochondria Recoupling Caused by Substrate Level Phosphorylation and Extramitochondrial Adenosine Phosphates. *European Journal of Biochemistry,61*(2), 551-561. doi:10.1111/j.1432-1033.1976.tb10050.x

Ricquier, D., & Bouillaud, F. (2000). Mitochondrial uncoupling proteins: From mitochondria to the regulation of energy balance. *The Journal of Physiology,529*(1), 3-10. doi:10.1111/j.1469-7793.2000.00003.x

Rimm, E. B., Stampfer, M. J., Giovannucci, E., Ascherio, A., Spiegelman, D., Colditz, G. A., & Willett, W. C. (1995). Body Size and Fat Distribution as Predictors of Coronary Heart Disease among Middle-aged and Older US Men. *American Journal of Epidemiology,141*(12), 1117-1127. doi:10.1093/oxfordjournals.aje.a117385

Rosenwald, M., Perdikari, A., Rülicke, T., & Wolfrum, C. (2013). Bi-directional interconversion of brite and white adipocytes. *Nature Cell Biology,15*(6), 659-667. doi:10.1038/ncb2740

Rousset, S., Alves-Guerra, M., Mozo, J., Miroux, B., Cassard-Doulcier, A., Bouillaud, F., & Ricquier, D. (2004). The Biology of Mitochondrial Uncoupling Proteins. *Diabetes,53*(Supplement 1). doi:10.2337/diabetes.53.2007.s130

Ràfols, M. E. (2014). Tejido adiposo: Heterogeneidad celular y diversidad funcional. *Endocrinología Y Nutrición,61*(2), 100-112. doi:10.1016/j.endonu.2013.03.011

Sacks, H., & Symonds, M. E. (2013). Anatomical Locations of Human Brown Adipose Tissue: Functional Relevance and Implications in Obesity and Type 2 Diabetes. *Diabetes,62*(6), 1783-1790. doi:10.2337/db12-1430

Santos, C. D., Balbo, S. L., Guimarães, A. T., Sagae, S. C., Negretti, F., & Grassiolli, S. (2017). Life-long Maternal Cafeteria Diet Promotes Tissue-Specific Morphological Changes in Male Offspring Adult Rats. *Anais Da Academia Brasileira De Ciências,89*(4), 2887-2900. doi:10.1590/0001-3765201720170316

Schulz, T., & Tseng, Y. (2013). Brown adipose tissue: Development, metabolism and beyond. *Biochemical Journal,453*(2), 167-178. doi:10.1042/bj20130457

Seale, P., Bjork, B., Yang, W., Kajimura, S., Chin, S., Kuang, S., Scimè, A., Devarakonda, S., Conroe, H. M., Erdjument-Bromage, H., Tempst, P., Rudnicki, M. A., Beier, D. R., Spiegelman, B. M. (2008). PRDM16 controls a brown fat/skeletal muscle switch. *Nature,454*(7207), 961-967. doi:10.1038/nature07182

Segovia, S. A., Vickers, M. H., Gray, C., & Reynolds, C. M. (2014). Maternal Obesity, Inflammation, and Developmental Programming. *BioMed Research International,2014*, 1-14. doi:10.1155/2014/418975

Shabalina, I., Petrovic, N., De Jong, J., Kalinovich, A., Cannon, B., & Nedergaard, J. (2013). UCP1 in Brite/Beige Adipose Tissue Mitochondria Is Functionally Thermogenic. *Cell Reports,5*(5), 1196-1203. doi:10.1016/j.celrep.2013.10.044

Sidossis, L., & Kajimura, S. (2015). Brown and beige fat in humans: Thermogenic adipocytes that control energy and glucose homeostasis. *Journal of Clinical Investigation,125*(2), 478-486. doi:10.1172/jci78362

Sullivan, E. L., Riper, K. M., Lockard, R., & Valleau, J. C. (2015). Maternal high-fat diet programming of the neuroendocrine system and behavior. *Hormones and Behavior,76*, 153-161. doi:10.1016/j.yhbeh.2015.04.008

Symonds, M. E., Pope, M., & Budge, H. (2012). Adipose tissue development during early life: Novel insights into energy balance from small and large mammals. *Proceedings of the Nutrition Society,71*(03), 363-370. doi:10.1017/s0029665112000584

Symonds, M. E. (2013). Brown Adipose Tissue Growth and Development. *Scientifica,2013*, 1-14. doi:10.1155/2013/305763

Symonds, M. E., Pope, M., & Budge, H. (2015). The Ontogeny of Brown Adipose Tissue. *Annual Review of Nutrition,35*(1), 295-320. doi:10.1146/annurev-nutr-071813-105330

Teruel, T., Valverde, A. M., Alvarez, A., Benito, M., & Lorenzo, M. (1995). Differentiation of rat brown adipocytes during late foetal development: Role of insulin-like growth factor I. *Biochemical Journal,310*(3), 771-776. doi:10.1042/bj3100771

Townsend, K. L., & Tseng, Y. (2014). Brown fat fuel utilization and thermogenesis. *Trends in Endocrinology & Metabolism,25*(4), 168-177. doi:10.1016/j.tem.2013.12.004

Trayhurn, P., & Jennings, G. (1987). Functional atrophy of brown adipose tissue during lactation in mice. Effects of lactation and weaning on mitochondrial GDP binding and uncoupling protein. *Biochemical Journal,248*(1), 273-276. doi:10.1042/bj2480273

Velickovic, K., Cvoro, A., Srdic, B., Stokic, E., Markelic, M., Golic, I., otasevic, V., Stancic, A., Jankovic, A., Vucetic, M., Buzadzic, B., Korac, B., Korac, A. (2014). Expression and Subcellular Localization of Estrogen Receptors α and β in Human Fetal Brown Adipose Tissue. *The Journal of Clinical Endocrinology & Metabolism,99*(1), 151-159. doi:10.1210/jc.2013-2017

Wang, Y., Beydoun, M. A., Liang, L., Caballero, B., & Kumanyika, S. K. (2008). Will All Americans Become Overweight or Obese? Estimating the Progression and Cost of the US Obesity Epidemic. *Obesity,16*(10), 2323-2330. doi:10.1038/oby.2008.351

Wilding, J. P. (2001). Causes of obesity. *Practical Diabetes International,18*(8), 288-292. doi:10.1002/pdi.277

Wright, S. M., & Aronne, L. J. (2012). Causes of obesity. *Abdominal Radiology,37*(5), 730-732. doi:10.1007/s00261-012-9862-x